JOURNAL OF SPACECRAFT AND ROCKETS
Vol. 31, No. 1, January–February 1994

Drag Reduction for Turbulent Flow over a Projectile: Part II

Shen-Min Liang*
National Cheng Kung University, Tainan, Taiwan, Republic of China
and
Jan-Kuang Fu†
Chinese Air Force Academy, Kangshan, Kaohsiung, Taiwan 82012, Republic of China

The performance of a secant-ogive-cylinder-boattail projectile in the transonic regime in terms of drag is numerically investigated. To improve the projectile performance, a drag reduction method, passive control of shock/boundary-layer interaction on the boattail, is applied. The effectiveness of this method is studied by varying the values of parameters such as porosity distribution, maximum porosity factor, and length of porous boattail section. The present results show that the passive control method applied on the boattail not only can reduce the boattail drag but also can reduce the base drag, and an additional 7% (approximately) total drag reduction is obtained compared with that without the passive control. The passive control effect on total drag reduction is found to be insensitive to Reynolds number.

Nomenclature

I_p = location of porous surface (porous boattail section)
$\bar{\sigma}$ = porosity distribution function in passive control
$\bar{\sigma}_{max}$ = maximum porosity

Introduction

IN Part I of this article, methods for reducing base drag evaluated were boattailing and base bleed or mass injection. Boattailing can effectively reduce the base drag since the base area and the extent of flow expansion at the base corner are reduced. For a projectile that flies at transonic speeds, there exists a shock that forms on the boattail portion and interacts with the boundary-layer. This shock interaction induces an additional wave drag that may be greater than the base drag for projectiles with large boattailed angles (say, $\beta > 5$ deg) and that reduces the boattailing effect on the total drag. This is a deficiency of this method and is neglected by most researchers. The second feasible method for reducing base drag is the use of base bleed, in which a small amount of mass flow is injected into the base region. Thus base bleed increases the base pressure and reduces the base drag. Although this method is very effective in reducing the base drag of projectiles, there exist at least three disadvantages in practical applications: 1) an active base bleed mechanism makes the projectile system more complicated; 2) additional power for pumping mass flow is required; and 3) the cost of a projectile with base bleed may be higher to manufacture.

The pressure drag on the boattail becomes a major contributor to the total drag for projectiles with larger boattailed angles. This is mainly due to the formation of a normal shock that induces an adverse pressure gradient on the boundary-layer. The interaction between the shock wave and the boundary layer is very complex. Thus, to improve the performance of a projectile with large boattailed angles, it is necessary to develop methods for reducing the drag, particularly on the boattail.

Received June 17, 1991; revision received Sept. 13, 1991; accepted for publication Sept. 24, 1991. Copyright © 1993 by S.-M. Liang. Published by the American Institute of Aeronautics and Astronautics, Inc., with permission.

*Associate Professor, Institute of Aeronautics and Astronautics. Member AIAA.
†Associate Professor, Department of Aeronautics.

In general, there are two methods available for the control of shock/boundary-layer interactions. The first is an active method[1-3] that uses either injection or suction in the region of shock/boundary-layer interaction to achieve a reduction in the pressure drag. This method reduces the shock strength and also avoids the occurrence of flow separation. However, strong injection not only thickens the boundary layer but also probably provokes an early separation as a side effect. An inadequate suction, on the other hand, might produce a stronger shock and may cause a higher wave drag as a negative effect. When an active control device is used, either injection or suction requires externally supplied power; thus, extra pumping drag should be added to the total drag of the body. An active method can be very effective if it is appropriately operated, however, it contains the same penalties as the base bleed technique. Namely, difficulties exist in the use of an active control primarily from the viewpoint of practical implementation and economic considerations.

The second method for control of shock/boundary-layer interaction is a passive control method which was originally suggested by Bushnell and Whitcomb and has been successfully applied to the drag reduction of transonic airfoils.[4-11] It has not been applied to transonic projectiles. An objective of this work is to study the passive control method for drag reduction of transonic projectiles. To the authors' knowledge, this is the first application of the passive control method of shock/boundary-layer interaction on projectiles.

The passive control of shock/boundary-layer interaction uses a porous surface and a cavity or submerged plenum located in the region of shock/boundary-layer interaction, as shown in Fig. 1. The static pressure rise across the shock wave results in a flow through the cavity from downstream to

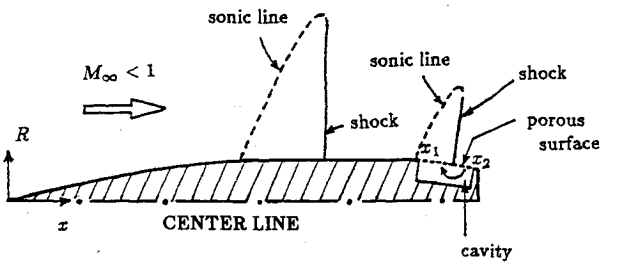

Fig. 1 Schematic of passive control of shock/boundary-layer interaction on boattail.

upstream of the shock wave. A passive control of shock/boundary layer interaction combines a passive downstream suction and a passive upstream injection for the shock. The cavity increases the communication of signals across the shock wave. The upstream injection leads to a rapid thickening of the boundary layer approaching the shock, which in turn produces a system of compression waves in an extended interaction region. This reduces the entropy increase, the energy loss, the pressure difference across the shock, and, consequently, the wave drag. The suction downstream of the shock not only avoids flow separation but also may reduce viscous losses. Past studies in the literature indicated that a porous surface and cavity can also damp out pressure fluctuations associated with shock-wave/boundary-layer interaction. The review paper of Raghunathan[12] provides more information about passive control of shock/boundary-layer interactions. Since both the suction and injection of the passive control method are done automatically, no active suction/injection mechanism and no additional power are required. Thus, the projectile system is simpler and easier to manufacture compared with that with an active control. Based on the previous arguments, a passive control technique appears to be a suitable candidate for drag reduction of a projectile with large boattail angles.

Mathematical Formulation and Numerical Methods

The equations and numerical procedure used to simulate the transonic turbulent flow past an axisymmetric projectile at zero angle of attack are given in Part 1.

Boundary Conditions

All boundary conditions are the same as those already described in Part I except for the permeable wall boundary condition on the boattail, which is described in the following section.

For the case of passive control over the boattail surface, the Darcy law employed by Chen et al.[8] is adopted in the present study. The Darcy law states that the transpiration velocity V_n through the porous wall is proportional to the pressure difference below and above the porous surface, i.e.,

$$V_n = -\sigma(p - \bar{p}) \tag{1a}$$

$$\sigma = \bar{\sigma}/(\rho_\infty U_\infty) \tag{1b}$$

where the subscript n denotes the outward direction normal to the surface; p is the pressure above the porous surface obtained from the flowfield, whereas $\bar{p}$ is the pressure below the porous surface that is assumed to be a constant; and $\bar{\sigma}$ is the porosity distribution function. For the passive flow through the cavity, the net mass through the porous surface of area S must be zero, or

$$Q = \int_S \rho V_n \, ds = 0$$

which gives, by assuming a constant cavity pressure and using Eq. (1),

$$\bar{p} = \frac{\int_S \sigma\rho p \, ds}{\int_S \sigma\rho \, ds} \tag{2}$$

Note that assumptions of constant cavity pressure and negligible energy loss in the cavity have been made but were found reasonably valid in airfoil applications.[6-8]

In this study, three types of porosity distribution will be examined by varying the porosity distribution function $\bar{\sigma}$ in Eq. (1b):

Type 1:

$$\bar{\sigma} = \bar{\sigma}_{\max} = \text{const} \tag{3a}$$

Type 2:

$$\bar{\sigma} = \bar{\sigma}_{\max}\sqrt{\sin\left(\frac{x - x_1}{x_2 - x_1}\pi\right)} \tag{3b}$$

where the parameters x_1 and x_2 are the limits of the porous boattail section as shown in Fig. 1, $\bar{\sigma}_{\max}$ is the maximum porosity which occurs at the midpoint of the porous section, and at the end points of the porous section the porous function $\bar{\sigma}$ is equal to zero.

Type 3:

$$\bar{\sigma} = \bar{\sigma}_{\max}\sqrt{\cos\left(\frac{\pi}{2}\frac{x - x_s}{x_k - x_s}\right)} \tag{3c}$$

where the parameter x_s is the horizontal position of the shock if the porous surface were solid, and x_k represents either x_1 or x_2, depending on whether x is less or greater than x_s. This function automatically adjusts the porosity distribution so that it decreases from the maximum value at the shock location to zero at either end of the porous section.

It can be seen that the type of porosity distribution $\bar{\sigma}$, the maximum porosity factor $\bar{\sigma}_{\max}$, and the length of porous section $I_p = (x_2 - x_1)$ are three factors in determining the effect of the passive control method on the drag reduction. For the porous wall on the boattail portion, the Cartesian velocity components are

$$u = V_n \cdot \sin\beta, \quad v = 0, \quad w = V_n \cdot \cos\beta \tag{4}$$

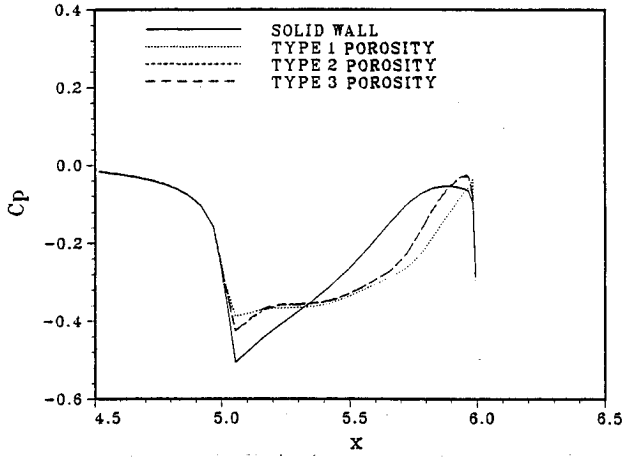

Fig. 2 Surface pressure distributions on the boattail of an SOCBT projectile for different types of porosity: $\bar{\sigma}_{\max} = 0.3$, $I_{p1} = [5.017, 5.968]$.

Results And Discussion

For projectiles with large boattailed angles, the pressure drag on the boattail portion may be greater than the base drag and becomes a major contributor to the total drag. The passive control of shock/boundary-layer interaction is applied to reduce the boattail drag. A 7-deg boattail-angle projectile at Mach number of 0.96 is chosen as a study case since a normal shock is located at about the middle of the boattail. The individual and combined effects of the parameters, porosity distribution, maximum porosity factor, and length of porous boattail section in the passive control on the drag reduction are explored. The influence of Reynolds number variation on porous effects is evaluated.

Effect of Porosity Distribution

To investigate the effect of porosity distribution on the base drag reduction, three types of porosity distribution are chosen and defined in Eqs. (3a-3c), respectively. The porous boattail section selected is in the interval between $x_1 = 5.017$ and $x_2 = 5.968$, denoted by I_{p1}, and three values of maximum

Table 1 Comparison of drag components and drag reduction with passive control method, $M_\infty = 0.96$, $\beta = 7$ deg, $I_{p1} = [5.017, 5.968]$

$\bar{\sigma}$	$\bar{\sigma}_{max}$	C_{DH}	C_{DV}	C_{DBT}	C_{DB}	C_{D0}	$\frac{\Delta C_{DBT}}{C_{DBT\,\mid Solid}}$[a]	$\frac{\Delta C_{DB}}{C_{DB\,\mid Solid}}$	$\frac{\Delta C_{D0}}{C_{D0\,\mid Solid}}$	$\frac{\Delta C_{D0}}{C_{D0\,\mid \beta=0}}$
Type 1	0.1	0.0290	0.0562	0.0935	0.0210	0.1997	0.016↓	0.382	0.058	0.252
	0.3	0.0290	0.0615	0.0981	0.0113	0.1998	0.033↑	0.668	0.058	0.251
	0.6	0.0292	0.0626	0.1033	0.0073	0.2024	0.087↑	0.785	0.045	0.242
Type 2	0.1	0.0291	0.0545	0.0896	0.0241	0.1973	0.057↓	0.291	0.069	0.259
	0.3	0.0291	0.0578	0.0925	0.0184	0.1979	0.026↓	0.459	0.067	0.258
	0.6	0.0292	0.0600	0.0972	0.0151	0.2013	0.023↑	0.556	0.050	0.246
Type 3	0.1	0.0292	0.0544	0.0900	0.0250	0.1986	0.053↓	0.265	0.063	0.256
	0.3	0.0292	0.0576	0.0933	0.0188	0.1990	0.018↓	0.447	0.061	0.254
	0.6	0.0291	0.0601	0.0975	0.0149	0.2016	0.026↑	0.562	0.049	0.245

[a]The symbol "↑" denotes increasing and "↓" denotes decreasing in quantity.

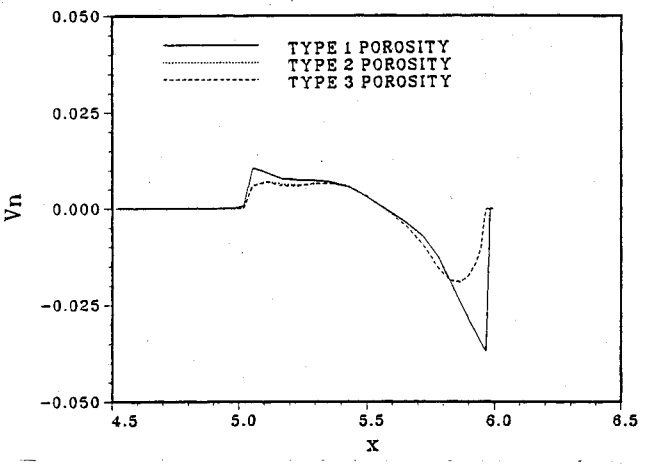

Fig. 3 Normal velocity distributions on boattail for different types of porosity: $\sigma_{max} = 0.3$, $I_{p1} = [5.017, 5.968]$.

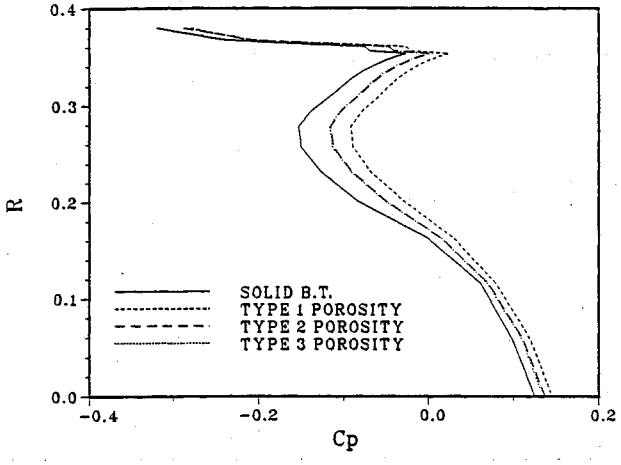

Fig. 4 Surface pressure distributions on base for different types of porosity: $\bar{\sigma}_{max} = 0.3$, $I_{p1} = [5,017, 5.968]$.

porosity factor ($\bar{\sigma}_{max} = 0.1$, 0.3, and 0.6) are chosen for the present study.

Figure 2 shows the computed distributions of pressure coefficient on the boattail of a secant-ogive-cylinder-boattail (SOCBT) projectile with $\bar{\sigma}_{max} = 0.3$. Compared with the result of no passive control, the pressure difference across the shock is reduced mainly because of the injection that thickens the boundary layer ahead of the shock and retards the expansion of the mainstream. The results indicate that the pressure distribution upstream of the porous interval is unaffected by the type of porosity. It is found that the pressure distributions on the boattail of the type 2 and type 3 porosity distributions are similar. The porous surface causes a weak shock wave near its upstream end ($x_1 = 5.017$), due to the injection from the cavity, and a normal shock on the boattail. The location of the normal shock is moved farther downstream because of the suction of air into the cavity, compared with that without passive control, in particular, for the type 1 porosity. Thus, for these three cases, the more aft the normal shock, the higher the pressure near the base corner. Figure 3 shows the normal velocity distributions on the boattail for different types of porosity. It can be seen that the type 1 (uniform) porosity distribution results in a stronger suction and a stronger injection than the type 2 and 3 cases. Moreover, the type 2 and 3 porosities produce almost the same distribution of normal velocity.

The predicted viscous drag for the type 1 case is larger than those of the other two types of porosity because stronger suction thins the boundary layer and results in a higher velocity gradient. Also, it was found that the viscous drag increases with maximum porosity factor.[13]

Figure 4 shows the surface pressure distributions on the base of an SOCBT projectile. Surprisingly, it is found that the base pressure is increased for all three types of porosity and that the base drag is significantly reduced. The type 1 porosity obtains a larger base drag reduction than the other two types of porosity. The reduction in base drag increases with maximum porosity factor and is about 67% for type 1 porosity with $\bar{\sigma}_{max} = 0.3$ and can be as high as 78% with $\bar{\sigma}_{max} = 0.6$ (see Table 1).

The variation of the boattail drag coefficient with maximum porosity factor was examined. The results indicated that the boattail drag increases with maximum porosity factor. The type 1 case obtains a greater boattail drag than the other two cases and even greater than that of the solid-boattail case. This is due to a stronger suction, producing a more downstream shock on the boattail and resulting in an increase in wave drag.

Table 1 provides results for the variation of the total drag coefficient with maximum porosity factor. It is found that a minimum in total drag is obtained when $\bar{\sigma}_{max} = 0.1$, and the type 2 porosity obtains a better performance than the other two types of porosity. Although the type 1 (uniform) porosity obtains a better base drag reduction, it also increases the boattail drag. For type 2 porosity with $\bar{\sigma}_{max} = 0.3$ case, an additional 7% reduction in total drag is obtained compared with that without passive control, and the net total drag reduction is about 26% compared with a zero-boattail-angle projectile.

Effect of Maximum Porosity Factor

All values of parameters used in this section remain the same as previously mentioned except that the porous interval is changed between $x_1 = 5.017$ to $x_2 = 5.864$, denoted by I_{p2}. Figure 5 shows the distributions of the pressure coefficient on the boattail of the SOCBT projectile with the type 2 porosity for different values of maximum porosity factor. It is seen that a larger value of maximum porosity factor produces a

Table 2 Comparison of drag components and drag reduction with passive control method, $M_\infty = 0.96$, $\beta = 7$ deg, $I_{p2} = [5.017, 5.864]$

$\bar{\sigma}$	$\bar{\sigma}_{max}$	C_{DH}	C_{DV}	C_{DBT}	C_{DB}	C_{D0}	$\frac{\Delta C_{DBT}}{C_{DBT\,\mid Solid}}$[a]	$\frac{\Delta C_{DB}}{C_{DB\,\mid Solid}}$	$\frac{\Delta C_{D0}}{C_{D0\,\mid Solid}}$	$\frac{\Delta C_{D0}}{C_{D0\,\mid\beta=0}}$
Type 1	0.1	0.0290	0.0545	0.0920	0.0233	0.1988	0.032	0.315	0.062	0.255
	0.3	0.0291	0.0560	0.0928	0.0205	0.1984	0.023	0.397	0.064	0.257
	0.6	0.0291	0.0573	0.0948	0.0184	0.1996	0.002	0.459	0.059	0.252
Type 2	0.1	0.0290	0.0537	0.0875	0.0255	0.1956	0.079	0.250	0.077	0.267
	0.3	0.0290	0.0548	0.0894	0.0230	0.1963	0.059	0.324	0.074	0.265
	0.6	0.0291	0.0563	0.0910	0.0218	0.1981	0.042	0.359	0.066	0.258
Type 3	0.1	0.0290	0.0535	0.0880	0.0263	0.1967	0.074	0.226	0.072	0.263
	0.3	0.0291	0.0550	0.0900	0.0233	0.1973	0.053	0.315	0.069	0.261
	0.6	0.0292	0.0563	0.0920	0.0213	0.1988	0.032	0.374	0.062	0.255

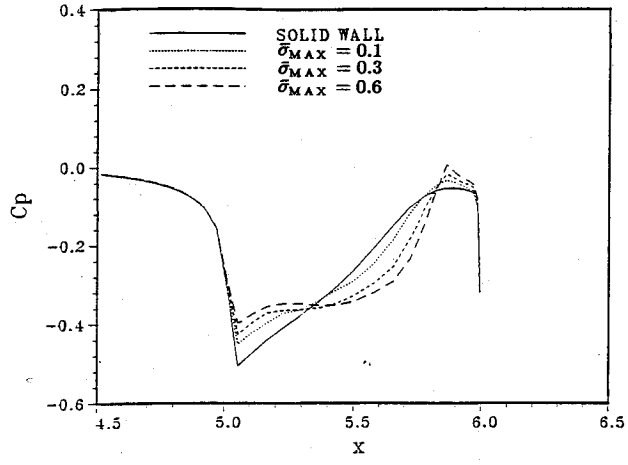

Fig. 5 Comparison of surface pressure distributions on boattail with type 2 porosity for different values of maximum porosity factor: $I_{p2} = [5.017, 5.864]$.

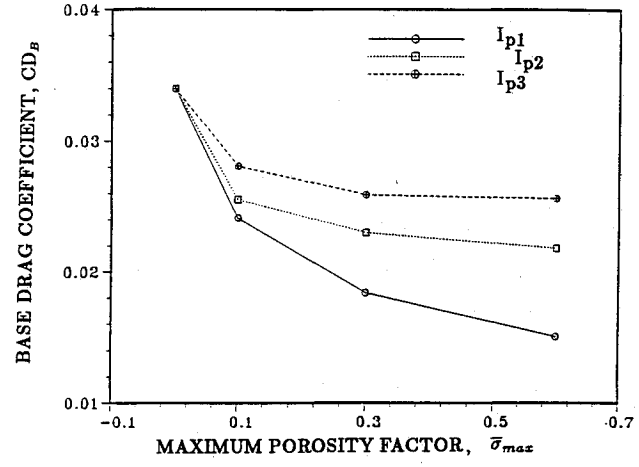

Fig. 7 Variation of base drag coefficient vs maximum porosity factor for different porous regions: type 2 porosity.

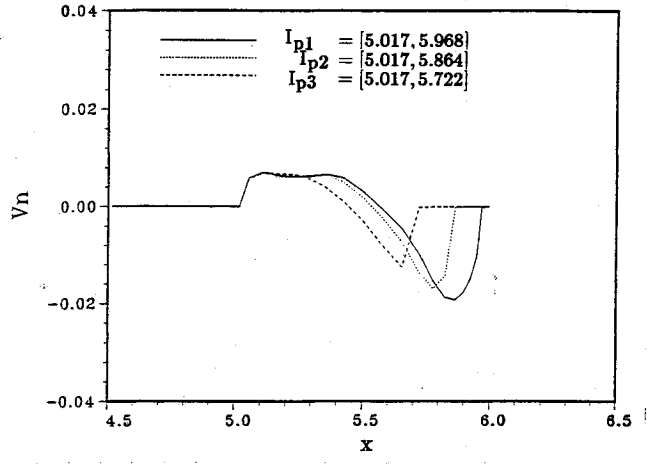

Fig. 6 Normal velocity distributions on boattail for different porous regions: $\bar{\sigma}_{max} = 0.3$, type 2 porosity.

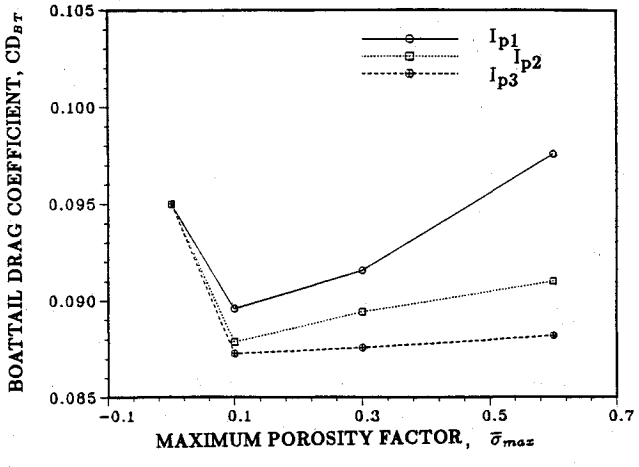

Fig. 8 Variation of boattail drag coefficient vs maximum porosity factor for different porous regions: type 2 porosity.

higher surface pressure upstream of the base corner because of stronger injection and suction ahead of and behind the normal shock, respectively. The stronger injection and suction for larger values of maximum porosity factor are known from the plot of normal velocity distributions on the boattail. For small values of maximum porosity factor, the resulting suction and injection are not effective and the location of the shock on the boattail changes very slightly, compared with the nonporous surface case. The pressure distribution upstream of the porous region was found to be unaffected by the maximum porosity factor.

The surface pressure distributions on the base for different values of maximum porosity factor were also examined. It was found that a larger value of maximum porosity factor provides a higher base pressure. Consequently, the larger the value of maximum porosity factor, the smaller the base drag, in particular, for the type 1 porosity (see Table 2). On the other hand, the boattail drag was found to increase with larger values of maximum porosity factor, especially for the type 1 porosity. The total drag is found to have a minimum at $\bar{\sigma}_{max} = 0.1$ for type 2 and 3 porosities and at $\bar{\sigma}_{max} = 0.3$ for type 1 porosity, as shown in Tables 1 and 2.

Effect of Length of Porous Boattail Section

In addition to the porous sections, I_{p1} and I_{p2}, used in the previous sections, a third interval, $I_{p3} = [5.017, 5.722]$, was

Table 3 Comparison of drag components and drag reduction with passive control method, $M_\infty = 0.96$, $\beta = 7$ deg, $I_{p3} = [5.017, 5.722]$

$\bar{\sigma}$	$\bar{\sigma}_{max}$	C_{DH}	C_{DV}	C_{DBT}	C_{DB}	C_{D0}	$\frac{\Delta C_{DBT}}{C_{DBT\,\mid Solid}}$[a]	$\frac{\Delta C_{DB}}{C_{DB\,\mid Solid}}$	$\frac{\Delta C_{D0}}{C_{D0\,\mid Solid}}$	$\frac{\Delta C_{D0}}{C_{D0\,\mid \beta=0}}$
Type 1	0.1	0.0292	0.0545	0.0891	0.0262	0.1990	0.062	0.229	0.061	0.254
	0.3	0.0292	0.0547	0.0896	0.0249	0.1983	0.057	0.268	0.065	0.257
	0.6	0.0291	0.0548	0.0902	0.0245	0.1986	0.051	0.279	0.063	0.256
Type 2	0.1	0.0291	0.0524	0.0873	0.0281	0.1968	0.081	0.174	0.072	0.263
	0.3	0.0291	0.0525	0.0876	0.0259	0.1951	0.078	0.238	0.080	0.269
	0.6	0.0291	0.0526	0.0882	0.0256	0.1955	0.072	0.247	0.078	0.268
Type 3	0.1	0.0290	0.0535	0.0872	0.0263	0.1960	0.082	0.226	0.076	0.266
	0.3	0.0290	0.0537	0.0873	0.0252	0.1952	0.081	0.259	0.080	0.269
	0.6	0.0291	0.0539	0.0877	0.0247	0.1953	0.077	0.274	0.079	0.268

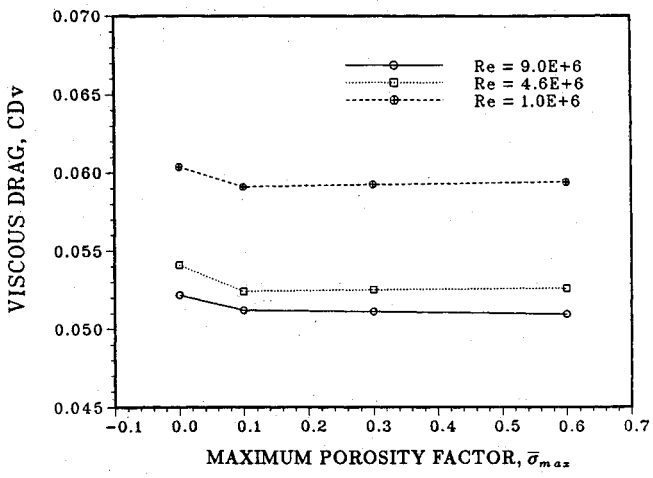

Fig. 9 Variation of viscous drag coefficient vs maximum porosity factor for different Reynolds numbers: type 2 porosity, $I_{p3} = [5.017, 5.722]$.

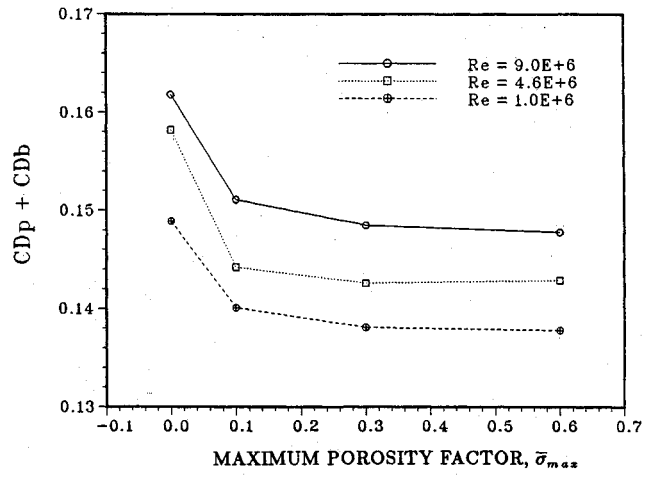

Fig. 10 Variation of sum of pressure drag and base drag coefficients vs maximum porosity factor for different Reynolds numbers: type 2 porosity, $I_{p3} = [5.017, 5.722]$.

also selected. The porosity distributions and the maximum porosity remain the same as before.

Figure 6 shows the normal velocity distribution on the boattail for different porous sections of type 2 porosity. It is seen that a longer porous section with its downstream end closer to the base corner produces a stronger suction behind the normal shock. Thus, a higher surface pressure (at $x = 5.95$) ahead of the base corner is obtained for the interval I_{p1}, since the shock location is closer to the base corner.

A comparison of the surface pressure distributions on the base was made and revealed that the longer porous section I_{p1} attains a higher base pressure and thus produces a larger base drag reduction. Figure 7 compares the variation of the base drag with maximum porosity factor for different porous sections. It is seen that the base drag decreases monotonically with maximum porosity factor but is most significantly decreased for the longest porous section I_{p1}. However, the longest porous section I_{p1} realizes a larger boattail drag for larger values of maximum porosity factor, as shown in Fig. 8. The results of Figs. 7 and 8 indicate that one can obtain an optimal value for the total drag depending on the length of porous section used. Note that a longer porous boattail section may induce the problem of projectile's stability and surface roughness that are not investigated in this study.

Tables 1–3 summarize drag components and drag reductions under the use of a passive control method for different porous sections. The best performance (the lowest total drag) is obtained for the case of type 2 porosity with maximum porosity factor ranging from 0.1 to 0.3. Small differences are found for the range of parameters investigated. The best performance is indicated in Table 3 for the case of type 2 porosity with maximum porosity factor of 0.3. This configuration realizes the following percent reductions compared with the geometry with no boattail: 8% for the boattail, 24% for the base, and 8% for the total drag.

Effect of Reynolds Number

The role of viscosity on passive control effectiveness was studied using the type 2 porosity distribution with the porous boattail section $I_{p3} = (5.017, 5.722)$ and three values of maximum porosity factor ($\bar{\sigma}_{max} = 0.1, 0.3$, and 0.6). Three different Reynolds numbers, $Re = 1.0 \times 10^6$, 4.6×10^6, and 9.0×10^6, were selected to evaluate porous effects on drag contributions. Figure 9 shows the viscous drag coefficient variation with the Reynolds number. The result indicates that the viscous drag C_{DV} decreases with increasing Reynolds number. The viscous drag coefficient for the case of 1.0×10^6 is about 10–14% greater than those in the other two cases and is almost independent of the maximum porosity factor. Figure 10 presents the variation of the sum ($C_{DP} + C_{DB}$) of the pressure drag and the base drag coefficients. It is found that the sum of C_{DP} and C_{DB} slightly increases with Reynolds number but is not significantly changed with the Reynolds number and the maximum porosity factor. The total drag coefficient was found to vary less than 2% over the range of Reynolds numbers investigated for a specified maximum porosity factor. Namely, the effect of the passive control is insensitive to Reynolds number.

Conclusion

To reduce the pressure drag on the boattail of a projectile with larger boattail angles, the passive control technique of shock/boundary-layer interaction is applied on the boattail and is proved to be an effective method. The present results show that the passive control method applied on the boattail not only can reduce the boattail drag but also can reduce the

base drag. The reduction in the boattail drag is due to the fact that the injection upstream of the shock reduces both the extent of flow expansion and the pressure difference across the shock and that the suction downstream of the shock makes the boundary layer thinner and avoids the susceptibility of flow separation. The reduction in base drag results from the effect of the suction that produces a more rearward shock location, leading to a higher surface pressure ahead of the base corner. It is found that the passive control technique provided approximately a 7% reduction in total drag, essentially independent of the type of porosity and the length of the porous boattail section for the range of maximum porosity factors 0.1–0.3. Porosity factors larger than 0.3 had an adverse effect on total drag reduction for the longest porous section investigated. The effect of passive control of the shock/boundary-layer interaction on total drag reduction is insensitive to Reynolds number.

References

[1]Krogmann, P., Stanewsky, E., and Thiede, P., "Effects of Suction on Shock/Boundary-Layer Interaction and Shock-Induced Separation," *Journal of Aircraft*, Vol. 22, No. 1, 1985, pp. 37–42.

[2]Thiede, P., "Supercritical Airfoil Flow Control by Slot Suction in the Shock Region," *Proceedings of the USAF/FRG DEA—Meeting on Viscous and Interacting Flowfield Effects*, AFFDL-TR-80-3088, Annapolis, MD, June 1980.

[3]Inger, G. R., and Zee, S., "Transonic Shockwave/Turbulent-Boundary-Layer Interaction with Suction or Blowing," *Journal of Aircraft*, Vol. 15, No. 11, 1978, pp. 750–754.

[4]Bahi, L., "Passive Shock Wave/Boundary Layer Control for Transonic Airfoil Drag Reduction," AIAA Paper 83-0137, Jan. 1983.

[5]Bahi, L., Ross, J. M., and Nagamatsu, T., "Passive Shock Wave/Boundary Layer Control for Transonic Aerofoil Drag Reduction," AIAA Paper 83-0137, Jan. 1983.

[6]Savu, G., and Trifu, O., "Porous Aerofoils in Transonic Flow," *AIAA Journal*, Vol. 22, No. 7, 1984, pp. 989–991.

[7]Nagamatsu, H. T., Orozco, R. D., and Ling, D. C., "Porosity Effect on Supercritical Airfoil Drag Reduction by Shock Wave/Boundary Layer Control," AIAA Paper 84-1682, June 1984.

[8]Chen, C. L., Chow, C. Y., Holst, T. L., and Van Dalsem, W. R., "Numerical Simulation of Transonic Flow over Porous Airfoils," AIAA Paper 85-5022, Oct. 1985.

[9]Chen, C. L., Chow, C. Y., Van Dalsem, W. R., and Holst, T. L., "Computation of Viscous Transonic Flow over Porous Aerofoils," AIAA Paper 87-0359, Jan. 1987.

[10]Nagamatsu, H. T., Dyer, R., Troy, N., and Ficarra, R. V., "Supercritical Aerofoil Drag Reduction by Passive Shock Wave/Boundary Layer Control in the Mach Number Range 0.75–0.9," AIAA Paper 85-0207, Jan. 1985.

[11]Lee, Y. C., "A Study on Aerodynamic Characteristics of Porous Airfoil," Master's Thesis, Inst. of Aeronautics and Astronautics, National Cheng Kung Univ., Tainan, Taiwan, ROC, 1989.

[12]Raghunathan, S., "Passive Control of Shock-Boundary Layer Interaction," *Progress in Aerospace Sciences*, Vol. 25, No. 3, 1988, pp. 271–296.

[13]Fu, J. K., "A Numerical Study on Drag Reduction of Turbulent Transonic Flow over a Projectile," Ph.D. Dissertation, Inst. of Aeronautics and Astronautics, National Cheng Kung Univ., Tainan, Taiwan, ROC, 1991.

Gerald T. Chrusciel
Associate Editor